

Structural intensity estimation via displacement and shape measurements of thin shells

Felipe PIRES⁽¹⁾, Stéphane AVRIL⁽²⁾, Steve VANLANDUIT⁽³⁾, Joris DIRCKX⁽⁴⁾

⁽¹⁾Universiteit Antwerpen & Vrije Universiteit Brussel, Belgium

⁽²⁾Mines Saint-Étienne, Université Lyon, France

⁽³⁾Universiteit Antwerpen & Vrije Universiteit Brussel, Belgium

⁽⁴⁾Universiteit Antwerpen, Belgium

Abstract

The structural intensity analysis on plates is a well-documented approach to identify energy paths taking place on a structure. By assuming that the sample behaves in accordance with the Kirchhoff-Love postulates, the structural intensity can be estimated by calculating spatial derivatives of the sample's out-of-plane displacement and by having a priori knowledge of its material properties. However, when shell-like structures are analyzed, the in-plane displacements become non-negligible terms and are critical inputs for the energy flow assessment. The purpose of this work is to present a method from which the energy transmission is estimated on the basis of full-field displacements and shape of arbitrary shells. This is dealt with by interpolating displacements fields on a finite element mesh that resembles the analyzed sample. After approximating these displacements on the nodes of that mesh and by treating the element's assembly as a Kirchhoff-Love plate model, the data differentiation via shape functions on predefined local coordinates is carried out. By having all differentiated data at hand, the structural intensity on thin shells is accessible. The method was validated from a model and it has shown itself to be a reliable tool to assess the vibrational energy in irregular shells.

Keywords: Structural intensity, Shell, Finite element, Energy transmission

1 INTRODUCTION

In the field of structural engineering, the Structural Intensity (SI) is a vector field that represents the energy transmission paths that takes place on a certain structure. The most common studies in this field are the vibrational energy flowing in simple structures, such as flat plates. Due to its simple geometry and by assuming that in-plane displacements are negligible, the SI can be assessed by computing 3rd spatial derivatives of out-of-plane displacements (1). It is no issue that these displacements were measured from the outer-surface, since they are considered to be constant throughout the direction normal of the plate's surface. However, if the SI of shell-like structures are to be assessed, then more inputs are required for further data processing. The in-plane displacements should be taken into account and these very fields may vary with respect to the sample's normal directions if the rotations are significant. These considerations become of importance if measurements can only be performed on a shell's outer-surface, which leads to additional data processing to estimate the relevant parameters from the shell's mid-surface. Not just several challenges were identified to assess the SI, but it is also from the author's knowledge that the SI analysis was done on shells with relatively simple geometries (2).

It is the aim of this work to present a method from which these issues are tackled for arbitrary shells and which takes into account both the membrane and bending strains. It is assumed that just the displacement data from a sample's outer-surface is at hand and that their vector components are not aligned with the local coordinates of the analyzed shell, as it is often the case on measurements. The dense spatial coordinates representing the shell are firstly used to develop a coarser Finite Element (FE) mesh composed with flat triangular elements. Afterwards, the raw displacements are projected on the nodes of that mesh (3) and their vector components are transformed, so they are aligned with a set of a local coordinate system. The strains are then computed via the differentiation of predefined and quadratic FE shape functions. After gathering all differentiated data

and by assuming that each element behaves in accordance with the Kirchhoff plate theory, data of the shell's mid-surface is estimated based the results obtained from the outer-surface. By having all the data at hand, the SI can be assessed.

A FE shell model was used to simulate a sample that would be measured. The data of its outer-surface was used to evaluate the obtained SI results from the proposed method and compare them with the energy transmission that is directly visible from the model. From this comparison, it could be seen that the reference and the estimated SI vector fields were in agreement with each other. Such results have shown that the method can deal with the major difficulties related to SI estimation.

2 THEORY

2.1 Structural intensity

It can be assumed that the contributions of in-plane displacements are negligible in the case of plates and that the SI is dominated by bending moments and shear forces (1). However, this assumption does not hold for irregular structures such as shells. Here, the membrane forces play an important role and they should also be taken into account when the vibrational energy is examined. By including this extra variable in the SI equations, the time-averaged and active SI [W/m^{-1}] on a shell's mid-surface and under an harmonic excitation is (4)

$$I_1 = -(\pi f) \Im \{ Q_1 u_3^* + M_{11} \theta_1^* + M_{12} \theta_2^* + N_{11} u_1^* + N_{12} u_2^* \} \quad (1)$$

and

$$I_2 = -(\pi f) \Im \{ Q_2 u_3^* + M_{21} \theta_1^* + M_{22} \theta_2^* + N_{21} u_1^* + N_{22} u_2^* \} \quad (2)$$

where the variables I_1 and I_2 are the SI vector components, the subscripts "1" and "2" are indications that the referred variables are oriented towards the orthogonal and in-plane directions of the specimen, the subscript "3" indicates that the term is aligned with respect to the direction normal to the shell's surface, the variables Q , M , N , u and θ are the vector components of the shear force \mathbf{Q} , bending moment \mathbf{M} , membrane force \mathbf{N} , displacement of the mid-surface \mathbf{u} and rotation $\boldsymbol{\theta}$, respectively; f is the frequency of excitation, " $\Im\{\}$ " denotes that just the imaginary unit of the referred term should be taken into account and the superscript "*" is the complex conjugate symbol.

The estimation of the generalized forces (\mathbf{Q} , \mathbf{M} and \mathbf{N}) and the rotation $\boldsymbol{\theta}$ depend on the assumptions being invoked to represent a shell's behavior. The choice of an appropriate theory to represent a sample was based on the final aim of this work: develop a method to estimate energy transmission paths on shells whose displacement fields and shape can only be measured from its outer-surface.

2.2 Kinematics of shells & generalized forces

The issue of developing a relationship between the data assigned to a shell's outer-surface (where measurements are made) and the desired variables on its mid-surface (region where the SI is estimated) was dealt with by assuming that the sample can be represented as a Kirchhoff-Love plate model. With this assumption, the specimen is treated as an assembly of flat plates each of which behaves in accordance with the Kirchhoff plate theory.

This simplification allows the out-of-plane displacement u_3 to be considered constant throughout the shell's normal direction. On the other hand, the in-plane displacements u_1 and u_2 vary linearly with respect to that very direction. Such variations occur due to the rotations θ_1 and θ_2 . Thus, the relation among the rotation $\boldsymbol{\theta}$, displacement of the mid-surface \mathbf{u} and the displacement of the outer-surface $\mathbf{u}^{h/2}$ can be expressed as

$$\mathbf{u} = \mathbf{u}^{h/2} - \frac{h}{2} \boldsymbol{\theta}, \quad (3)$$

being h the sample's thickness. The individual vector components of eq.(3) are organized as

$$\mathbf{u} = \begin{Bmatrix} u_1 \\ u_2 \\ u_3 \end{Bmatrix}, \quad \mathbf{u}^{h/2} = \begin{Bmatrix} u_1^{h/2} \\ u_2^{h/2} \\ u_3^{h/2} \end{Bmatrix}, \quad \boldsymbol{\theta} = \begin{Bmatrix} \theta_1 \\ \theta_2 \\ 0 \end{Bmatrix}. \quad (4)$$

By invoking the infinitesimal strain theory, the strains can be computed with

$$\varepsilon_{ij} = \frac{1}{2}(u_{i,j}^{h/2} + u_{j,i}^{h/2}), \quad \chi_{ij} = \frac{1}{2}(\theta_{i,j} + \theta_{j,i}), \quad \text{for } i, j = \{1, 2\}, \quad (5)$$

where ε and χ are defined as components of the strain of the outer-surface $\boldsymbol{\varepsilon}$ and the bending strain $\boldsymbol{\chi}$, respectively; and the subscripts “ i ” and “ j ” indicate that the mentioned field is differentiated along those directions. The components of the mentioned strains are organized as follows:

$$\boldsymbol{\varepsilon} = \begin{Bmatrix} \varepsilon_{11} \\ \varepsilon_{22} \\ \varepsilon_{12} \end{Bmatrix}, \quad \boldsymbol{\chi} = \begin{Bmatrix} \chi_{11} \\ \chi_{22} \\ \chi_{12} \end{Bmatrix}. \quad (6)$$

The strains also vary linearly with respect to the through-thickness coordinate due to the Kirchhoff plate theory. Therefore, the strain on the outer-surface ($\boldsymbol{\varepsilon}$) and the one on the mid-surface ($\boldsymbol{\gamma}$) can be related to each other with the following equation:

$$\boldsymbol{\gamma} = \boldsymbol{\varepsilon} - \frac{h}{2}\boldsymbol{\chi}. \quad (7)$$

Lastly, the generalized forces \mathbf{N} and \mathbf{M} are defined and related to the membrane strain $\boldsymbol{\gamma}$ and bending strain $\boldsymbol{\chi}$, respectively. The shear force \mathbf{Q} can be assessed from the equilibrium condition of a differential element, which leads to a relation of \mathbf{Q} with spatial derivatives of \mathbf{M} . All these equations are presented next:

$$\mathbf{N} = \begin{Bmatrix} N_{11} \\ N_{22} \\ N_{12} \end{Bmatrix} = h\mathbf{C}\boldsymbol{\gamma}, \quad \mathbf{M} = \begin{Bmatrix} M_{11} \\ M_{22} \\ M_{12} \end{Bmatrix} = \frac{h^3}{12}\mathbf{C}\boldsymbol{\chi}, \quad \mathbf{Q} = \begin{Bmatrix} Q_1 \\ Q_2 \end{Bmatrix} = \begin{Bmatrix} M_{11,1} + M_{12,2} \\ M_{12,1} + M_{22,2} \end{Bmatrix}. \quad (8)$$

The term \mathbf{C} represents the stiffness matrix, which can be interpreted in terms of the Young's modulus E and Poisson coefficient ν :

$$\mathbf{C} = \frac{E}{1-\nu^2} \begin{bmatrix} 1 & \nu & 0 \\ \nu & 1 & 0 \\ 0 & 0 & 1-\nu \end{bmatrix}. \quad (9)$$

2.3 Requirements of the Finite Element mesh

It has been stated that the analyzed shell can be represented as an assembly of flat plates. Due to this assumption, the shape of the specimen should be simplified but to a degree that its overall shape is still preserved. Since it is the aim of this research to use this methodology on several irregular shapes, it was decided to use flat triangular elements.

The displacement \mathbf{u} is stored on the nodes of this FE mesh and the order of the elements depend on the derivative's order needed for this application. The membrane force and bending moment can be assessed by differentiating the displacement and rotation [see eq.(5)], respectively. However, the shear force is dependent on the 1st order derivative of the \mathbf{M} components, which in turn depend on 2nd order derivatives of the rotation $\boldsymbol{\theta}$. Due to this requirement, it was chosen to develop a FE mesh with flat triangular elements of the quadratic type (“linear strain triangle” elements).

2.4 Data projection & estimation of the rotation

There are 2 issues that should be addressed before projecting measured displacement data on a developed FE mesh. The first one is related to the spatial coordinates where the measured displacement fields are stored: it is highly probable that those locations do not coincide in number and position with the nodes of the developed FE mesh. The second problem is related to the coordinate system with which these measured displacements are represented: they are probably not equal to a set of a local coordinate system defined in Sections 2.1 and 2.2, i.e., the triad $(\mathbf{e}_1, \mathbf{e}_2, \mathbf{e}_3)$.

These issues were dealt with by projecting the measured data with a global least-squares minimization algorithm (3) and by transforming the coordinate system with which the displacements are represented. To simulate a dense point cloud of experimental data, it was assumed that their spatial coordinates were not equal in number or position with the nodes of a coarse FE and quadratic mesh. Moreover, the raw displacement fields were represented with respect to a Cartesian coordinate set $(\mathbf{e}_x, \mathbf{e}_y, \mathbf{e}_z)$. This displacement field is referred here to as $\mathbf{U}_{\text{exp}}^{h/2}$.

The projection of the displacement field $\mathbf{U}_{\text{exp}}^{h/2}$ to the nodes of a mesh is computed with (3)

$$\mathbf{U}^{h/2} = \left[[\Phi^T \Phi]^{-1} \Phi^T \right] \mathbf{U}_{\text{exp}}^{h/2}, \quad (10)$$

where Φ is the assembled matrix of the quadratic shape functions evaluated at the coordinates of $\mathbf{U}_{\text{exp}}^{h/2}$ and $\mathbf{U}^{h/2}$ is the displacement stored on the nodes of the mesh.

After acquiring the displacement field $\mathbf{U}^{h/2}$, the rotation represented with the same coordinate system $(\mathbf{e}_x, \mathbf{e}_y, \mathbf{e}_z)$ can also be estimated. This field is represented here as Θ and it is computed by subtracting the vectors normal to the sample's surface under its deformed configuration ($\bar{\mathbf{e}}_3$) with the ones of the reference mesh (\mathbf{e}_3) (5). The equation that represent this procedure is

$$\Theta = \bar{\mathbf{e}}_3 - \mathbf{e}_3. \quad (11)$$

2.5 Overview of the method

The presented method contains several steps towards the assessment of the SI. Table 1 presents an overview of all steps that are necessary: from the projection of the raw displacement field (Step 1) to the evaluation of the vibrational energy (Step 6).

Table 1. Steps towards assessing the SI

Steps	Description
1	Project the $\mathbf{U}_{\text{exp}}^{h/2}$ to the nodes of the mesh [eq.(10)]
2	Compute the rotation Θ [eq.(11)]
3	Transformation of coordinates: $\mathbf{U}^{h/2}, \Theta \rightarrow \mathbf{u}^{h/2}, \theta$
4	Calculate the required spatial derivatives [eqs.(5, 8)]
5	Compute the parameters related to the mid-surface [eqs.(3, 7)]
6	Assess the structural intensity [eqs.(1, 2)]

3 Results

The validation of the current method was tested on a FE shell model, from which the correct SI could be visualized. The model was set to behave in accordance with the Mindlin-Reissner theory, which enables the model to present the shear strains ε_{13} and ε_{23} . Those strains are neglected in the Kirchhoff-Love plate model and, thus, this comparison will be able to show if the equations in Section 2.2 are too restrictive.

The shape of the model was based on a real cone-like sample (Figure 1 (a)). Fixed boundary conditions were applied to its free edges and a viscous damper (represented in blue in the same Figure) was applied on its

center. Also, a uniform and harmonic pressure of 1 Pa and at 50 Hz was applied on all the shell's domain with the exception of the damped region. By developing such a model, predictable energy transmission paths that flow towards the damper are generated. Lastly, the thickness, Young's modulus and Poisson coefficient of the shell model were set to be 1 mm, 8 MPa and 0.3, respectively.

After the simulation's completion, a dense point cloud of the shell's outer-surface that contained the displacement field aligned with the Cartesian coordinates $\mathbf{U}_{\text{exp}}^{h/2}$ was exported for further processing (Figure 1 (b)).

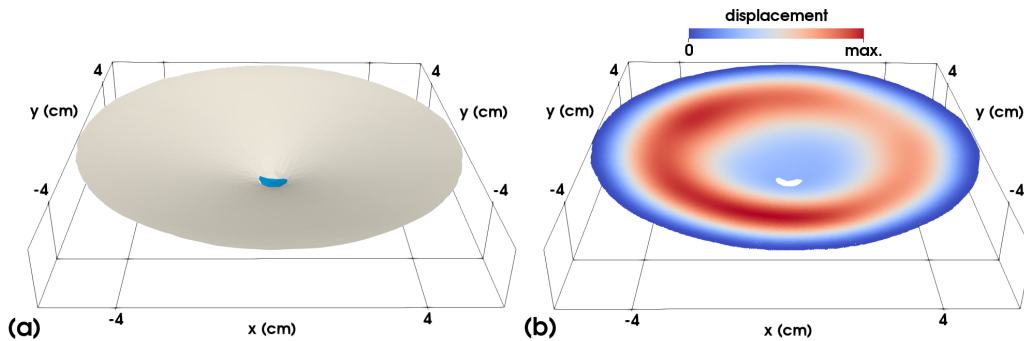


Figure 1. (a): Geometry of the shell model. The surfaces represented in blue are the boundaries where the damper was applied. The gray zones are excited with a uniform and harmonic pressure. (b): Dense point cloud (76,000 evaluated points) of the computed displacement fields. The colored fields represent the u_z field as an example.

The next step consists in creating a FE mesh with quadratic elements, where the $\mathbf{U}_{\text{exp}}^{h/2}$ would be projected to. The quadratic mesh is displayed in Figure 2 (a). Afterwards, eq.(10) was used to project the densely populated displacement $\mathbf{U}_{\text{exp}}^{h/2}$ [Figure 1 (b)] to the mesh's nodes. The colored field in Figure 2 (a) presents the field $\mathbf{U}^{h/2}$ on the nodes of the mesh and Figure 2 (b) shows a chosen set of local coordinates \mathbf{e}_1 and \mathbf{e}_2 for further processing.

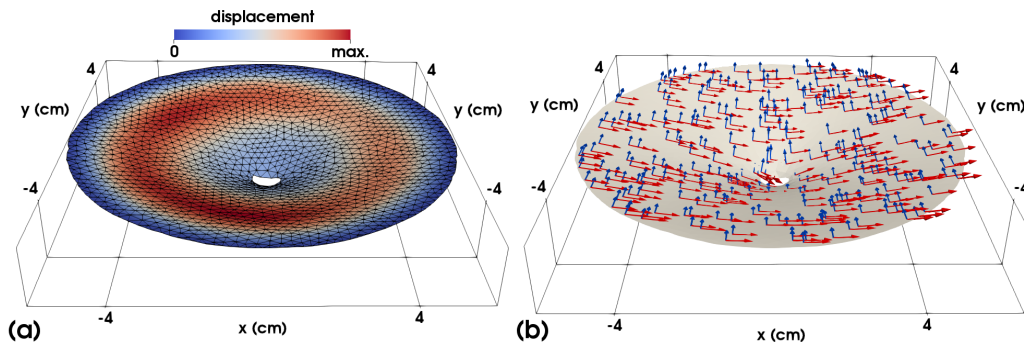


Figure 2. (a): Developed FE mesh with quadratic elements and 7,000 nodes. The colored fields represent the z-component of $\mathbf{U}^{h/2}$. (b): Chosen set of local coordinates \mathbf{e}_1 (red arrows) and \mathbf{e}_2 (blue arrows). The 3rd direction \mathbf{e}_3 is normal to the shell's surface and they point upwards.

At this step, the displacement $\mathbf{U}^{h/2}$ is at hand and the steps described in Table 1 (steps 3 to 6) can be followed, so the variables related to the SI can be visualized for validation. Figure 3 (a) presents the SI results that are directly acquirable from the FE model and Figure 3 (b) displays the results obtained from the proposed method.

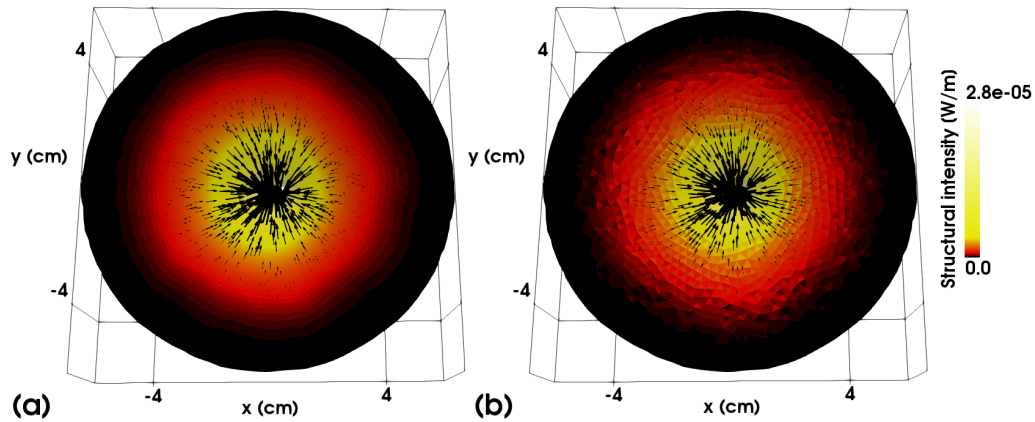


Figure 3. (a): SI vector field that is computed directly from the model. The colored field on the shell represents the SI magnitudes. (b): SI that was assessed from the presented method. The vectors and colored field have the same meaning as the ones shown in “(a)”.

4 CONCLUSIONS

The SI that was obtained from the proposed method [Figure 3 (b)] showed results that were in agreement with the energy paths that can be directly computed in the model [Figure 3 (a)]. Such statement is valid for both the vector directions of the vibrational energy (represented in with black vectors) and their magnitudes (represented as a colored field on the shell). It is also worth noting that the shear strains related to the normal directions (ε_{13} and ε_{23}) are neglected in the Kirchhoff-Love plate model. This strong assumption is absent in the shell model, which behaves in accordance with the Reissner-Mindlin theory and takes the mentioned strains into account.

Even though stronger assumptions were used to develop the equations described in this work (Section 2.2), the method was still able to extract the correct vibrational energy values. These preliminary results shows that the method was able to deal with the challenges of assessing the parameters present on a shell’s mid-surface just by taking the information related to sample’s outer-surface into account. The presented work was considered to be validated from this test and, next, it will be implemented on real shell-like structures.

ACKNOWLEDGMENTS

Financial support for this work was supplied by the Research Foundation of Flanders (FWO), (Grant No. G049414N).

REFERENCES

- [1] Lamberti, A.; Semperlotti, F. Detecting closing delaminations in laminated composite plates using nonlinear structural intensity and time reversal mirrors. *Smart Materials and Structures*, Vol. 22 (12), 2013, p. 125006.
- [2] Saijyou, K.; Yoshikawa, S. Structural intensity measurement of cylindrical shell based on NAH technique and influences of a rib on the acoustic energy flow. *Journal of the Acoustical Society of Japan (E)*, Vol. 20(2), 1999, p. 125-136.
- [3] Avril, S.; Pierron, F.; General framework for the identification of constitutive parameters from full-field measurements in linear elasticity. *International Journal of Solids and Structures*, Vol. 44 (14-15), 2007, p. 4978-5002.

- [4] Gavrić, L.; Pavić, G. A finite element method for computation of structural intensity by the normal mode approach. *Journal of sound and vibration*, Vol. 164 (1), 1993, p. 29-43.
- [5] Wagner, W.; Gruttmann, F. A simple finite rotation formulation for composite shell elements. *Engineering Computations*, Vol. 11 (2), 1994, p. 145-176.